

## Probabilistic analysis of seismically isolated elevated liquid storage tank using multi-phase friction bearing

Hesamaldin Moeindarbari<sup>1</sup>, Masoud Malekzadeh<sup>2</sup> and Touraj Taghikhany<sup>\*1</sup>

<sup>1</sup>Department of Civil and Environmental Engineering, AmirKabir University of Technology (Polytechnic), Tehran, Iran

<sup>2</sup>Department of Civil, Environmental and Construction Engineering, University of Central Florida, Orlando, Florida, USA

(Received April 30, 2013, Revised July 15, 2013, Accepted October 23, 2013)

**Abstract.** Multiple level performance of seismically isolated elevated storage tank isolated with multi-phase friction pendulum bearing is investigated under totally 60 records developed for multiple level seismic hazard analysis (SLE, DBE and MCE). Mathematical formulations involving complex time history analysis have been proposed for analysis of typical storage tank by multi-phase friction pendulum bearing. Multi-phase friction pendulum bearing represent a new generation of adaptive friction isolation system to control super-structure demand in different hazard levels. This isolator incorporates four concave surfaces and three independent pendulum mechanisms. Pendulum stages can be set to address specific response criteria for moderate, severe and very severe events. The advantages of a Triple Pendulum Bearing for seismic isolation of elevated storage tanks are explored. To study seismic performance of isolated elevated storage tank with multi-phase friction pendulum, analytical simulations were performed with different friction coefficients, pendulum radii and slider displacement capacities.

**Keywords:** multi-phase friction pendulum; probabilistic analysis; seismically isolated elevated storage tank; demand parameter

### 1. Introduction

Storage tanks are considered as infrastructures since they are strategically important. Fractures of such structures have immense vital effect on people's life, such as fire or environmental contamination when flammable materials or hazardous chemicals seep out (e.g., 1960 Chile (Steinbrugge and Rodrigo 1963), 1978 Izu-Oshima and Miyagi (Minowa 1980), 1971 San Fernando, and 1987 Whittier earthquakes (Knoy 1995)). Consequently earthquake protection for such facilities has attracted serious attention in the industrial and engineering communities. Seismic isolation system is conceivably one of the most promising alternatives to mitigate the transmitted inertial force from the substructure to the superstructure of isolated storage tanks (Malhotra 1997, Wang *et al.* 2001, Jadhav and Jangid 2006, Christovasilis and Whittaker 2008). Seismic isolation can separate the tank (or any other type of structure) from the harmful motions of the ground by providing flexibility and energy dissipation capability through the insertion of the

---

\*Corresponding author, Ph.D., E-mail: [ttaghikhany@aut.ac.ir](mailto:ttaghikhany@aut.ac.ir)

so-called isolators between the foundation and the superstructure. Primary isolation devices are categorized into elastomeric-based and frictional/sliding-based isolators. Behavior and characteristics of these two seismic isolation devices are provided in previous studies. Despite of the most regular structures for which the designated weight remains constant over the life span of structure, storage tanks weight varies in time. What makes Friction Pendulum Systems (FPS) desirable for seismic isolation of storage tanks is the fact that the FPS design procedure is independent of the structure weight while it plays crucial role in design of structures isolated with electrometric systems.

Advantages of frictional based seismic devices for isolation of storage tanks lead to a large number of researches in this field of study. Frictional based isolation systems can be applied for a pervasive frequency input; therefore they can seize the opportunity to avoid the risk of resonance. Hence electrometric-based devices are not a decent approach for seismic isolation of storage tanks. Frictional based isolation (particularly FPS) can fully meet the requirements of storage tank seismic isolation demand.

For the first time, in an uncommon application, seismic isolation was proposed for the rehabilitation of several elevated storage tanks in Seattle (Bleiman and Kim 1993). Shenton and Hampton carried out a numerical investigation and concluded that the seismic isolation technique can effectively reduce the earthquake response of the elevated tanks especially for those with low capacity or high height-to-diameter ratios (Shenton and Hampton 1999). Shrimali and Jangid in 2003 performed a thorough study on the response of the slender and broad isolated elevated fluid storage tanks considering two different methods for isolating the tanks (Shrimali and Jangid 2003). They demonstrated that the base shear, which was mainly dominated by the impulsive and rigid mass components, could be significantly reduced due to the isolation. Likewise, it was indicated that the peak sloshing displacement of the slender tanks increase as a result of isolation effect while no such effect was observed for broad tanks. The dilemma with regard to the FPS and other conventional isolation systems is the requirement of large amount of damping to mitigate very rare displacements which can be detrimental to the performance of the structures under occasional and rare events (Kelly 1999). The above-mentioned dilemma can be solved by recent developments in the design and manufacturing of FPS bearings. The development has centered on the use of multiple pendulum mechanisms to exhibit different hysteretic properties at different stages of displacement response and enhances seismic performance of seismically isolated storage tanks by exhibiting multi-stage behavior (Makris and Vassiliou 2011, Malekzadeh and Taghikhany 2010, 2012). Double-concave friction pendulum (DCFP) bearing as the first generation of multiple pendulum bearings, has two sliding surfaces and its hysteretic model can be derived by considering two FPS bearings in series (Fenz and Constantinou 2006). Sonia *et al.* investigated the behavior of liquid storage slender and broad tanks isolated by the double variable frequency pendulum isolator (DVFPI). The DVFPI is a double sliding isolation system having elliptical sliding surfaces. They found that the performance of the DVFPI can be optimized by designing the sliding surfaces and the coefficient of friction for broad tanks (Sonia *et al.* 2011).

Newly developed class of multiple pendulum bearings called Triple Pendulum Bearing (TPB) exhibits improved hysteretic characteristic to control the performance over broad range of excitations (Morgan 2007, Morgan and Mahin 2007, Fenz and Constantinou 2008a, 2008b, 2008c) (See Fig. 1). TPB enables engineers to choose different combination of stiffness and damping in different levels of excitation and achieve multiple performance objectives, which were not accessible in the past.

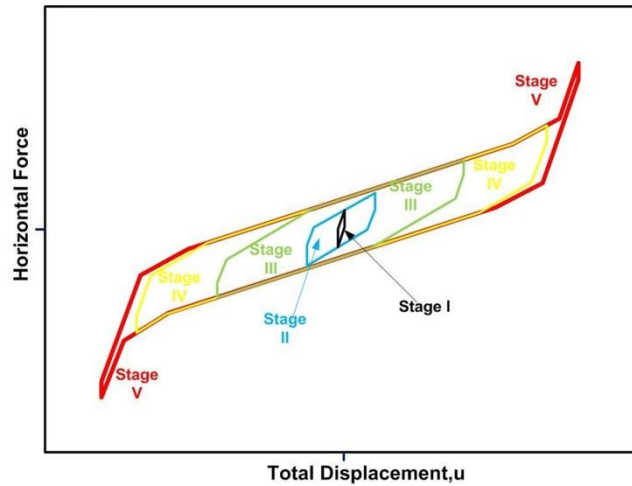


Fig. 1 Different stages of sliding related to adaptive TPB

The purpose of this paper is to study the multi level performance of elevated storage tank using multi-stage friction pendulum focused on a triple pendulum system. Mathematical formulation involving complex time history analysis have been proposed for analysis of a typical storage tank by triple pendulum bearing subjected to ensembles of ground motions developed for multiple levels of seismic hazard (SLE, DBE & MCE). A parametric study carried out to show the advantages of Triple Pendulum Bearing to Single Pendulum Bearings (SPB).

## 2. Adaptive triple pendulum bearing

The results of attempts to enhancing the performance of single friction pendulum bearing (FPS) leads to the introduction of a new generation of adaptive friction isolation systems called multi spherical bearings. The behaviors of these bearings are termed as adaptive because they progressively exhibit different hysteretic properties at different stages of displacement. The stiffness and damping can be changed to predictable values at different controllable amplitudes. These properties let the design of isolation system to be separately optimized in multiple levels of input excitation. As it is shown in Fig. 2,  $R_i$  is the radius of curvature of surface  $i$ ,  $h_i$  is the radial distance between the pivot point and surface  $i$  and  $\mu_i$  is the coefficient of friction at the sliding interface. The internal construction of these bearings permits sliding on different combinations of surfaces throughout the course of motion, resulting in changes in stiffness and damping (Fenz and Constantinou 2008a).

Here, in order to investigate seismic performance of elevated storage tanks using TPB, a generic model comprises the sloshing, impulsive, and rigid masses in terms of liquid mass and TPB bearing are considered. Different stages of sliding related to TPB during different levels of excitation have been illustrated. These stages are defined as follow (see Fig. 2):

*Stage I:* Sliding on surface 2 and 3 only, this stage forms one pendulum mechanism, and defines the properties of the isolation system under low levels of excitation (Service Level Earthquake: SLE).

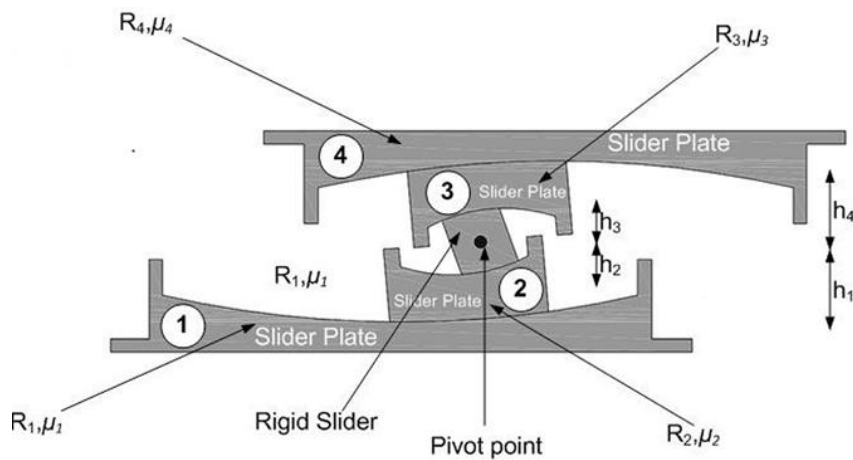


Fig. 2 Section of a TPB

*Stage II:* Motion stops on surface 2; sliding on surface 1 and 3. This mechanism defines the primary properties of the isolation system under moderate levels of excitation (Design Basis Earthquake: DBE).

*Stage III:* Motion stopped on surface 2 and 3; sliding on surface 1 and 4. The friction coefficient of upper concave (surface 4) is sufficiently large to prevent sliding until an extreme level of excitation occurs (Maximum Credible Earthquake: MCE).

*Stage IV:* Slider contacts restrainer on surface 1; motion remains stopped on surface 3; sliding on surface 2 and 4. This mechanism defines properties of isolation bearing beyond MCE.

*Stage V:* Slider bears on restrainer of surface 1 and 4; sliding on surface 2 and 3 (final stage).

### 3. Mathematical model of seismically isolated elevated liquid storage tank using TPB

#### 3.1 Series model of TPB

The hysteretic behavior of this novel isolation system can be simulated by series model of three independent friction pendulum elements (Fenz and Constantinou 2008c). Any friction pendulum element in this model includes three parallel parts, including a linear elastic spring, a rigid plastic spring for accounting the friction, and a gap element. Gap element provides considerable restrain stiffness beyond the displacement capacity. The small mass of articulated slider and sliding plate are describe by  $M_{slider1}$  and  $M_{slider2}$ . The reason to consider these small masses is to find displacements and velocities on each concave individually and formulate their equations of motion.

#### 3.2 Mathematical formulation

Fig. 3 shows the six-degree-of-freedom structural model of isolated elevated liquid storage tank. In this model, the interaction between the fluids with the tank wall is represented by a

mass-spring-damper system. The fluid is replaced by sloshing, impulsive, and rigid lumped masses,  $m_c, m_i$ , and  $m_r$ , respectively, associated with  $u_c, u_i$ , and  $u_r$  degrees of freedom, in the same order. The first two masses are connected to the tank wall by two equivalent springs having stiffness constants  $k_c$ , and  $k_i$ , and two equivalent dampers having damping constants  $c_c$ , and  $c_i$ , respectively. The tank geometrical parameters are liquid height  $H$ , radius  $R$ , and average thickness of tank wall,  $t_r$ . The value of three above mentioned discrete masses and the associated natural frequencies of sloshing and impulsive masses,  $\omega_c$  and  $\omega_i$ , can be expressed as below (Haroun 1983)

$$m_c = Y_c m_f \quad (1)$$

$$m_i = Y_i m_f \quad (2)$$

$$m_r = Y_r m_f \quad (3)$$

$$\omega_c = \sqrt{1.84 \left( \frac{g}{R} \right) \tanh(1.84S)} \quad (4)$$

$$\omega_i = \frac{P}{H} \sqrt{\frac{E}{\rho_s}} \quad (5)$$

$$m_f = \pi R^2 H \rho_w \quad (6)$$

Where  $S = H/R$  is the tank aspect ratio, and  $E$ , and  $\rho_s$  are modulus of elasticity and density of tank wall, respectively. Also, the values of  $Y_c, Y_i, Y_r, P$  parameters, supposing  $t_r/R = 0.004$ , are described in Eq. (7) (Haroun 1983)

$$\begin{Bmatrix} Y_c \\ Y_i \\ Y_r \\ P \end{Bmatrix} = \begin{bmatrix} 1.01327 & -0.8757 & 0.35708 & 0.06692 & 0.00439 \\ -0.15467 & 1.21716 & -0.62839 & 0.14434 & -0.0125 \\ -0.01599 & 0.86356 & -0.30941 & 0.04083 & 0 \\ 0.037085 & 0.084302 & -0.05088 & 0.012523 & -0.0012 \end{bmatrix} \begin{Bmatrix} 1 \\ S \\ S^2 \\ S^3 \\ S^4 \end{Bmatrix} \quad (7)$$

The equivalent stiffness and damping of sloshing and impulsive masses can be obtained as

$$K_c = m_c \omega_c^2 \quad (8)$$

$$K_i = m_i \omega_i^2 \quad (9)$$

$$c_c = 2\xi_c m_c \omega_c \quad (10)$$

$$c_i = 2\xi_i m_i \omega_i \quad (11)$$

Where  $\xi_c$  and  $\xi_i$  are the damping ratio of sloshing and impulsive masses, respectively.

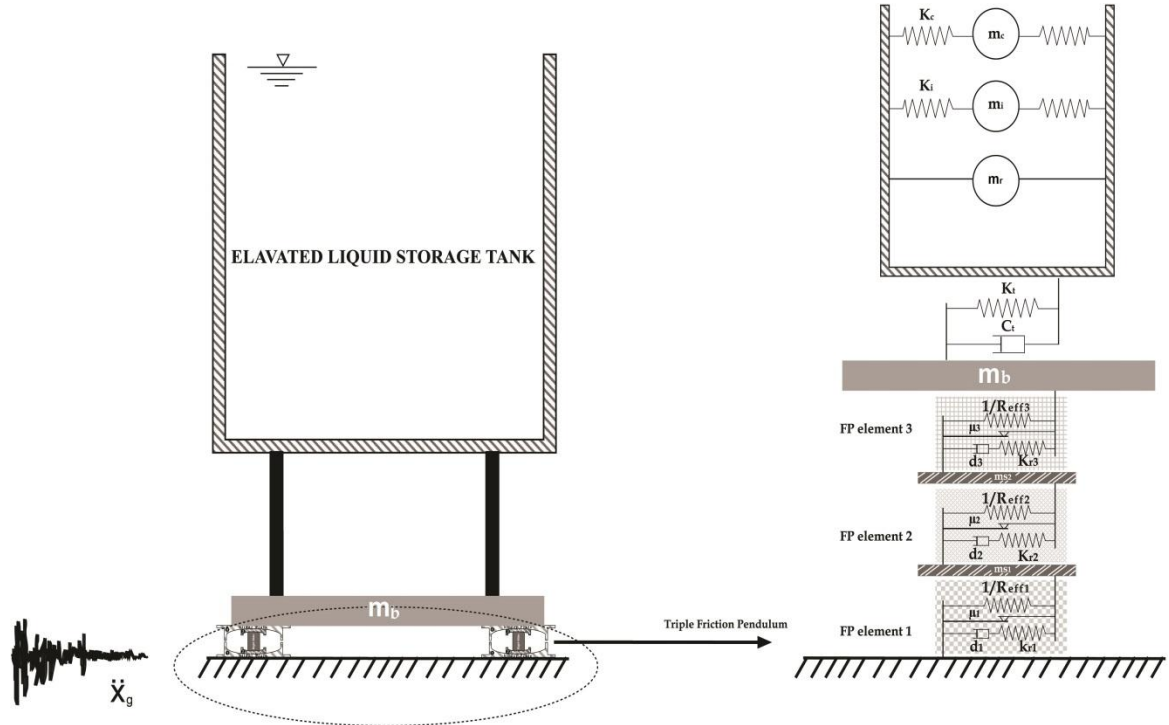


Fig. 3 Six-degree-of-freedom structural model of isolated elevated liquid storage tank

### 3.3 Governing equation of motion

In this study, based on a review of past investigations, the mass of tank supporting tower structure,  $m_{st}$ , is supposed to be 10 percent of the fluid mass  $m_f$ . In fact, 75 percent of that mass is associated with  $u_t$  degree of freedom while 25 % is corresponded with  $u_b$  degree of freedom. Finally, the natural period of full tank, which is a fixed-base structure,  $T_t$ , is assumed to be equal to 1.0 sec. The stiffness of tower structure can be obtained as  $k_t = 4\pi^2(m_c + m_i + m_r + 0.075m_f)/T_t^2$ . Likewise, the mass of isolation system  $M_b$  is considered to be constant and equal to 10 % of the fluid mass along the study. Writing the equilibrium equations of exerted forces on tank masses, considering that the displacements of tank degrees-of-freedom are relative to the ground, the six below equations can be readily derived as

$$m_c(\ddot{u}_c + \ddot{u}_g) + k_c(u_c - u_t) + c_c(\dot{u}_c - \dot{u}_t) = 0 \quad (12)$$

$$m_i(\ddot{u}_i + \ddot{u}_g) + k_i(u_i - u_t) + c_i(\dot{u}_i - \dot{u}_t) = 0 \quad (13)$$

$$\begin{aligned} (m_r + 0.075m_f)(\ddot{u}_t + \ddot{u}_g) + k_c(u_t - u_c) \\ + k_i(u_t - u_i) + k_t(u_t - u_b) + c_c(\dot{u}_t - \dot{u}_c) \\ + c_i(\dot{u}_t - \dot{u}_i) + c_t(\dot{u}_t - \dot{u}_b) = 0 \end{aligned} \quad (14)$$

$$(m_b + 0.025m_f)(\ddot{u}_b + \ddot{u}_g) + k_t(u_b - u_t) + c_t(\dot{u}_b - \dot{u}_t) + F_{FPS3} = 0 \quad (15)$$

$$m_{s2}(\ddot{u}_{s2} + \ddot{u}_g) + F_{FPS2} - F_{FPS3} = 0 \quad (16)$$

$$m_{s1}(\ddot{u}_{s1} + \ddot{u}_g) + F_{FPS1} - F_{FPS2} = 0 \quad (17)$$

Where  $m_{s1}$  and  $m_{s2}$  are the slider masses and its value is kept fixed and equal to 5 kg throughout the study.  $F_{FPS1}$ ,  $F_{FPS2}$  and  $F_{FPS3}$  are the developed resisting forces in lower, inner and upper concave surfaces due to ground motions, respectively, described as

$$F_{FPS1} = \frac{(m_f + m_b + m_{s1} + m_{s2})g}{R_{eff1}}(x_{s1}) + \mu_1(m_f + m_b + m_{s1} + m_{s2})gZ_1 + K_{r1}(|x_{s1}| - d_1)\text{sign}(x_{s1})H(|x_{s1}| - d_1) \quad (18)$$

$$F_{FPS2} = \frac{(m_f + m_b + m_{s2})g}{R_{eff2}}(x_{s2} - x_{s1}) + \mu_2(m_f + m_b + m_{s2})gZ_2 + K_{r2}(|x_{s2} - x_{s1}| - d_2)\text{sign}(x_{s2} - x_{s1})H(|x_{s2} - x_{s1}| - d_2) \quad (19)$$

$$F_{FPS3} = \frac{(m_f + m_b)g}{R_{eff3}}(x_b - x_{s2}) + \mu_3(m_f + m_b)gZ_3 + K_{r3}(|x_b - x_{s2}| - d_3)\text{sign}(x_b - x_{s2})H(|x_b - x_{s2}| - d_3) \quad (20)$$

Where  $K_{ri}$  is the stiffness exhibited by the displacement restrainers and  $d_i$  is the displacement capacity of surface  $i$ .  $H$  is the Heaviside step function.  $\mu_i$  is the velocity dependent coefficients of friction and can be obtained as

$$\mu_1 = \mu_{\max 1} - (\mu_{\max 1} - \mu_{\min 1}) \exp(-a_1 |\dot{x}_{s1}|) \quad (21)$$

$$\mu_2 = \mu_{\max 2} - (\mu_{\max 2} - \mu_{\min 2}) \exp(-a_2 |\dot{x}_{s2} - \dot{x}_{s1}|) \quad (22)$$

$$\mu_3 = \mu_{\max 3} - (\mu_{\max 3} - \mu_{\min 3}) \exp(-a_3 |\dot{x}_b - \dot{x}_{s2}|) \quad (23)$$

$\mu_{\max}$  and  $\mu_{\min}$  are, respectively the sliding coefficients of friction at maximum and minimum velocity of sliding and  $a$  is a constant parameter and its value is suggested as 100 sec/m for interfaces consisting of polished stainless steel and the PTFE composite. And finally,  $Z_i$  is hysteretic variables ranging between -1 and 1 that is governed by following differential equation

$$\frac{dZ_1}{dt} = \frac{1}{u_{y1}} \{A_1 - |Z_1|^n [\gamma_1 \text{sgn}(\dot{x}_{s1})Z_1 + \beta_1]\}(\dot{x}_{s1}) \quad (24)$$

$$\frac{dZ_2}{dt} = \frac{1}{u_{y2}} \left\{ A_2 - |Z_2|^{\eta_2} \left[ \gamma_2 \operatorname{sgn}((\dot{x}_{s2} - \dot{x}_{s1})Z_2) + \beta_2 \right] \right\} (\dot{x}_{s2} - \dot{x}_{s1}) \quad (25)$$

$$\frac{dZ_3}{dt} = \frac{1}{u_{y3}} \left\{ A_3 - |Z_3|^{\eta_3} \left[ \gamma_3 \operatorname{sgn}(\dot{x}_b - \dot{x}_{s2})Z_3 + \beta_3 \right] \right\} (\dot{x}_b - \dot{x}_{s2}) \quad (26)$$

Where  $u_{yi}$  is the yield displacement.  $\gamma_i$ ,  $\beta_i$ ,  $\eta_i$  and  $A_i$  are dimensionless variables that control the shape of the hysteresis loop. Above-equations are solved simultaneously for each time step using the *ode15s* solver in MATLAB programming language in order to obtain the time history of tank seismic response (Shampine and Reichelt 1997).

#### 4. Earthquake ground motions

Study presented here set goals for investigated multi-stage performance of seismically isolated elevated storage tank using TPB over different hazard levels. Achieving this goal require ground motion time history related to multiple hazard levels. As a part of SAC steel Project, suites of time histories to use in performance based-design were generated (Somerville *et al.* 1998). Suites of time history are provided at three probabilities of occurrence: SLE (50% in 50 year), DBE (10% in 50 year) and MCE (2% in 50 year) and developed for Boston, Seattle and Los Angeles which represent a range of seismic hazard levels from seismic Zone 2 to Zone 4. These records have a wide variety of intensities and frequency content, providing an effective mean of studying multi-stage performance of TPB and comparing structures over different hazards. So in this study the suite of 60 time histories developed for Los Angeles used as input to nonlinear dynamic analysis. Table 1 list the characteristic of records used in this study. Figure 4 illustrates 5% damped absolute acceleration response spectra for SLE, DBE and MCE level. Median response acceleration for each group is depicted by red line.

#### 5. Numerical study and results

In the present study the effects of TPBs bearings are examined on the earthquake response of isolated elevated liquid storage tanks, namely slender tank. The characteristics of this tank are: (i) the aspect ratio,  $S$  for slender tank is 1.85 (ii) the height,  $H$ , of water filled in the slender tank is 10 m and (iii) the ratio of tank wall thickness to its radius,  $t_r/R$ , is taken to be 0.004. The natural frequencies of sloshing and impulsive mass are 0.291 and 6.738 Hz. The tank wall is steel with modulus of elasticity,  $E = 200$  GPa and a mass density,  $\rho_s = 7900$  kg/m<sup>3</sup>.

To show the effectiveness of TPB over SPB in different seismic hazard levels, analytical simulation conducted using ensembles of ground motions developed for multiple levels of seismic hazard. Two different seismically isolated elevated storage tanks were investigated in this study, one isolated with Single Pendulum Bearing (SPB), and the other one with Triple Pendulum Bearing (TPB). In order to have a fair comparative study between two types of bearings, TPB characteristics are selected by using two following approaches:

a) Design isolation systems to exhibit approximately the same “displacement” under MCE ground motions (Set 1),

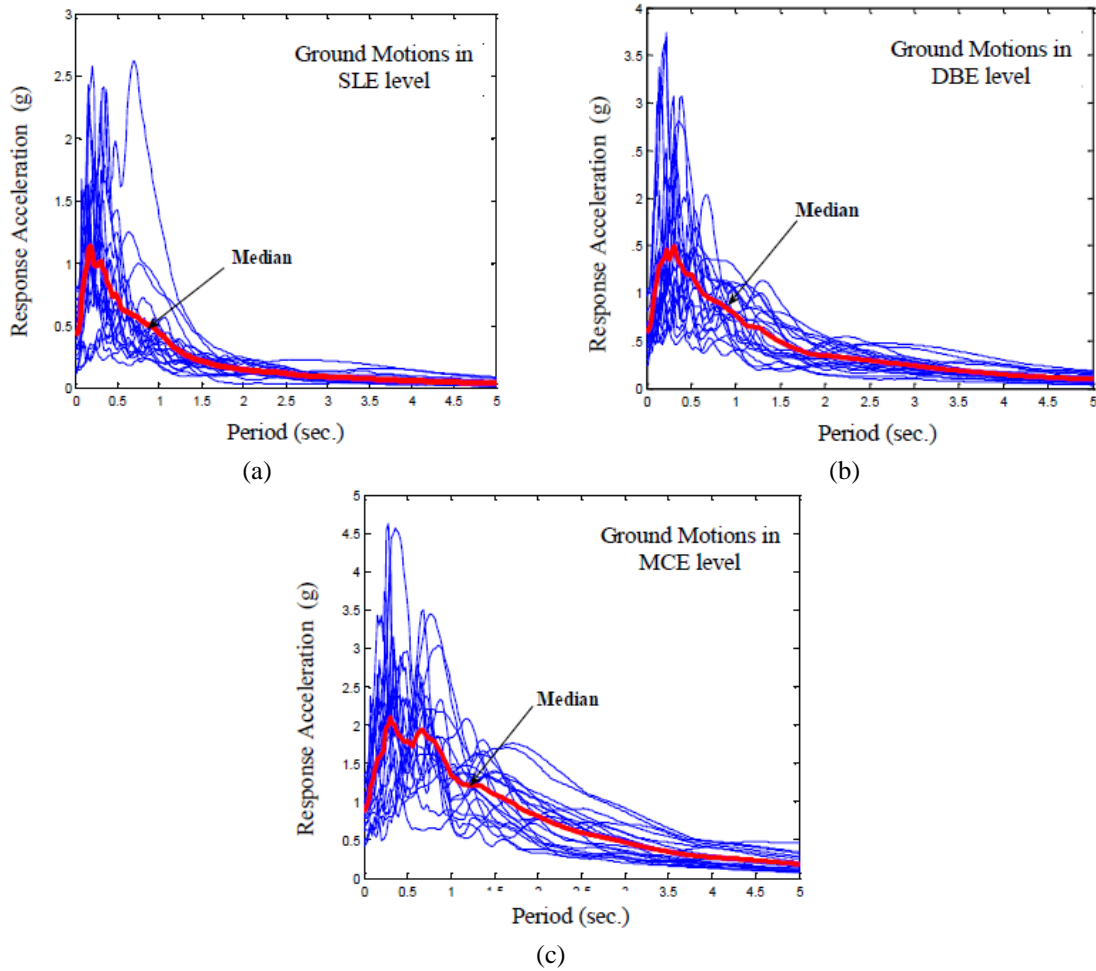


Fig. 4 Response acceleration spectra of time histories ensembles

b) Design isolation systems to exhibit the same “strength” (same force at zero displacement) and the same “second” slope in hysteretic behavior (Set 2). To have same force at zero displacement the “static friction coefficients” of surfaces 2 and 3 in TPB should be equal to the “static friction coefficient” of the sliding surface in SPB system. Moreover both isolation systems were designed to exhibit the same second effective stiffness (period or slope). The effective stiffness of SPB systems is equal to  $W/R_{eff}$ , where  $R_{eff}$  is the effective radius of curvature for the SFP system. In TPB systems (Fig. 1) at the second slope, the sliding occurs on surfaces 2 and 3 and the effective stiffness of the system is equal to  $W/(R_{eff2} + R_{eff3})$ . So as Table 2 shows, the characteristics of two isolation bearings, designed in a way that  $1/(R_{eff2} + R_{eff3})_{TPB} = 1/(R_{eff})_{SPB}$ .

The nonlinear time-history analysis is conducted using precise mathematical model (mentioned in section 5) for both systems under ensembles of ground motions (60 records in three categories: SLE, DBE and MCE). The response quantities of interest are tower shear force (measured at top of the isolation system), sloshing displacement,  $u_c - u_t$  and bearings displacement relative to the ground,  $u_b$ .

Table 1 Multiple hazard levels ground motions

SLE			DBE			MCE		
Record	Amplitude	Record	Amplitude	Record	Amplitude	Record	Amplitude	
Label	Name	Scale Factor	Label	Name	Scale Factor	Label	Name	Scale Factor
LA41	Coyote Lake	0.59	LA01	Imperial Valley	0.461	LA21	Artificial	1.283
LA42	Coyote Lake	0.333	LA02	Imperial Valley	0.676	LA22	Artificial	0.921
LA43	Imperial Valley	0.143	LA03	Imperial Valley	0.393	LA23	Artificial	0.418
LA44	Imperial Valley	0.112	LA04	Imperial Valley	0.488	LA24	Artificial	0.473
LA45	Kern County	0.144	LA05	Imperial Valley	0.302	LA25	Northridge	0.868
LA46	Kern County	0.159	LA06	Imperial Valley	0.234	LA26	Northridge	0.944
LA47	Landers	0.337	LA07	Landers	0.421	LA27	Northridge	0.927
LA48	Landers	0.308	LA08	Landers	0.426	LA28	Northridge	1.33
LA49	Morgan Hill	0.318	LA09	Landers	0.52	LA29	Tabas	0.809
LA50	Morgan Hill	0.546	LA10	Landers	0.36	LA30	Tabas	0.992
LA51	Parkfield	0.781	LA11	Loma Prieta	0.665	LA31	Artificial	1.297
LA52	Parkfield	0.632	LA12	Loma Prieta	0.97	LA32	Artificial	1.297
LA53	Parkfield	0.694	LA13	Northridge	0.678	LA33	Artificial	0.782
LA54	Parkfield	0.791	LA14	Northridge	0.657	LA34	Artificial	0.681
LA55	North Palm	0.518	LA15	Northridge	0.533	LA35	Artificial	0.992
LA56	North Palm	0.379	LA16	Northridge	0.58	LA36	Artificial	0.101
LA57	San Fernando	0.253	LA17	Northridge	0.569	LA37	Artificial	0.712
LA58	San Fernando	0.231	LA18	Northridge	0.817	LA38	Artificial	0.776
LA59	Whittier	0.769	LA19	North Palm	1.019	LA39	Artificial	0.5
LA60	Whittier	0.478	LA20	North Palm	0.987	LA40	Artificial	0.657

Fig. 5 shows an example of a time history response of a slender tank isolated with SPB and TPB (Set1 and Set2) bearings under Imperial Valley, 1979 (El Centro Array #5) earthquake ground motion. The maximum bearing displacement for TPB Set1, TPB Set2 and SPB cases are 16.19, 23.33 and 24.49 cm, respectively. In addition, the peak tower shear force and sloshing displacement with using SPB bearing are 27.74 and 17.24 percent higher than the maximum responses of tower with TPB sets, respectively. As seen in figure, relative advantage of two sets of TPBs to each other depends on the selected demand parameters. For example TPB Set 1 has lower maximum bearing displacement while TPB Set 2 is preferred in controlling the maximum tower shear force and sloshing displacement.

Table 2 Characteristics of proposed TPB sets and SPB

Classification	Surface No.	Friction Coefficient		Effective Radius of Curvature (m)
		$\mu_{min}$	$\mu_{max}$	
TPB (Set 1)	1	0.04	0.08	1.522
	2	0.01	0.02	0.4
	3	0.01	0.02	0.4
	4	0.09	0.18	1.522
TPB (Set 2)	1	0.08	0.016	5.791
	2	0.06	0.12	1.522
	3	0.06	0.12	1.522
	4	0.09	0.18	5.791
SPB	-	0.06	0.12	3.04

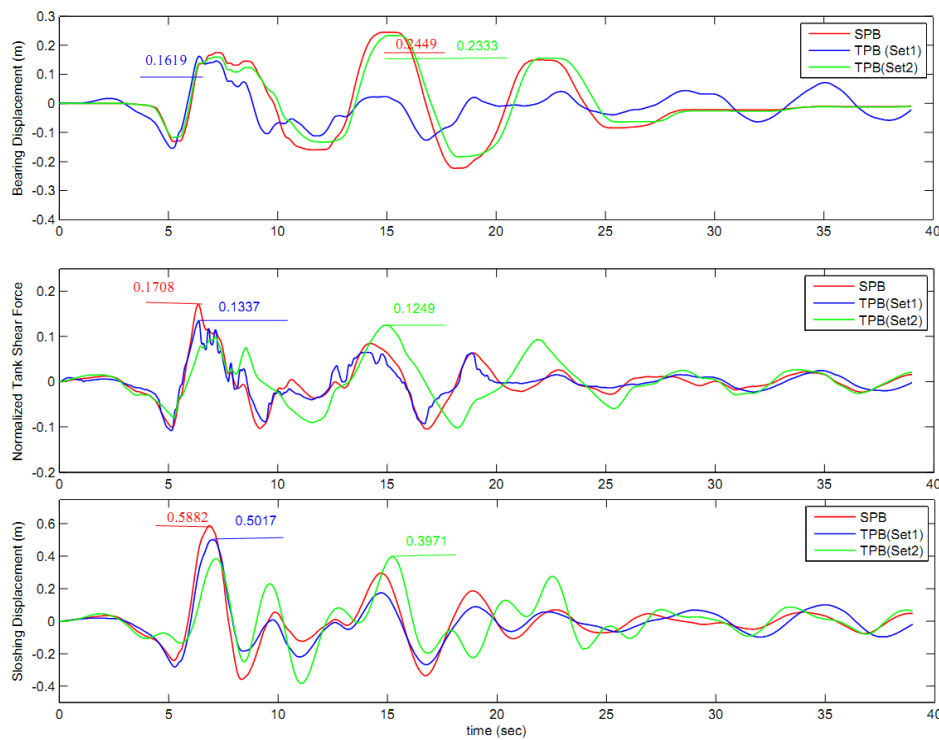
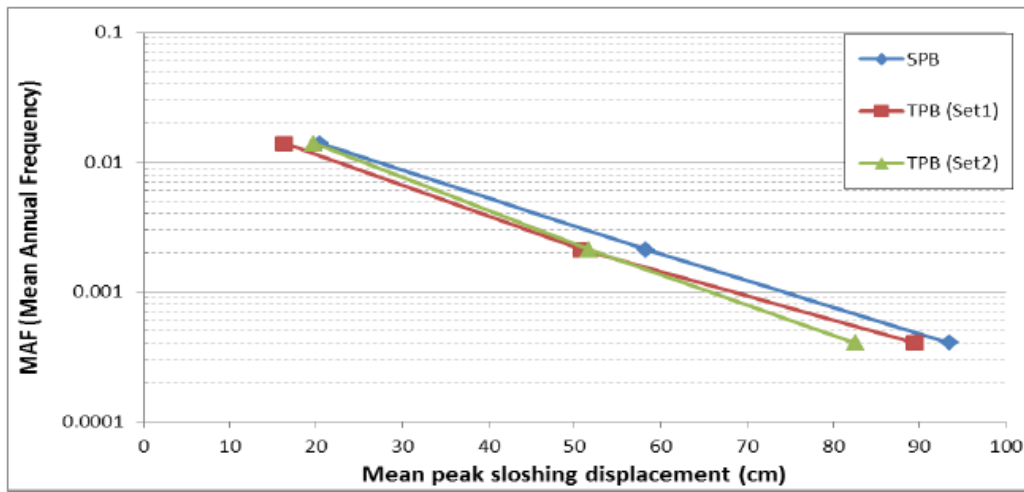


Fig. 5 An example of a time history response of the slender tank isolated with SPB and TPB(Set 1 and Set2) under Imperial Valley, 1979 (El Centro Array #5) earthquake ground motion

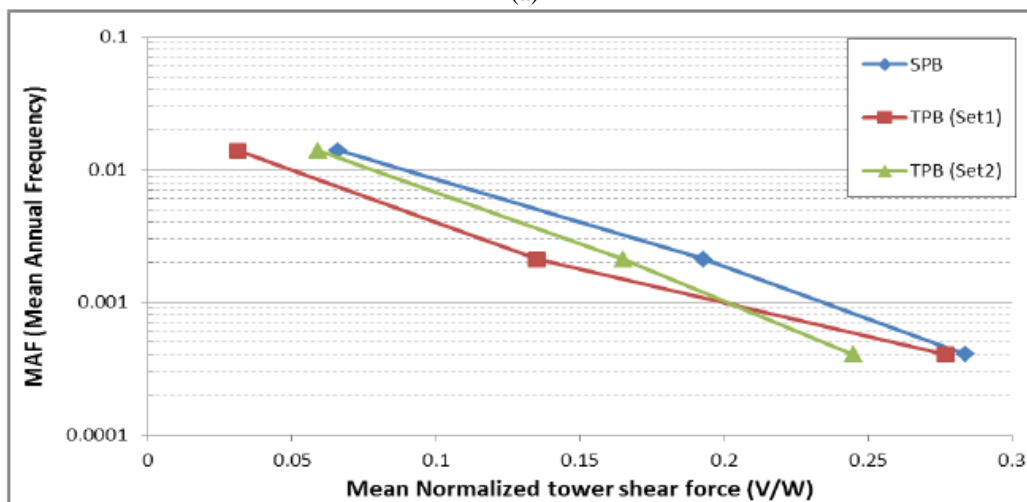
Here, in order to have a thorough knowledge of the subject, it is necessary to compare the average peak responses of tower with two types of bearings under the ground motions in Table 1. Accordingly for each level of hazard, the median demand of three parameters is listed in Table 3 and their demand hazard curves are plotted in Fig. 6.

Table 3 Mean peak quantities of interest under three different hazard level

Seismic hazard level	Isolation type	Mean peak sloshing displacement (cm)	Mean Normalized tower shear force (V/W)	Mean peak isolation displacement (cm)
SLE	SPB	20.43	0.066	12.45
	TPB (Set1)	16.33	0.031	9.35
	TPB (Set2)	19.80	0.059	12.67
DBE	SPB	58.33	0.193	25.35
	TPB (Set1)	50.86	0.135	20.42
	TPB (Set2)	51.70	0.165	27.30
MCE	SPB	93.45	0.284	31.78
	TPB (Set1)	89.47	0.277	29.32
	TPB (Set2)	82.60	0.245	39.45

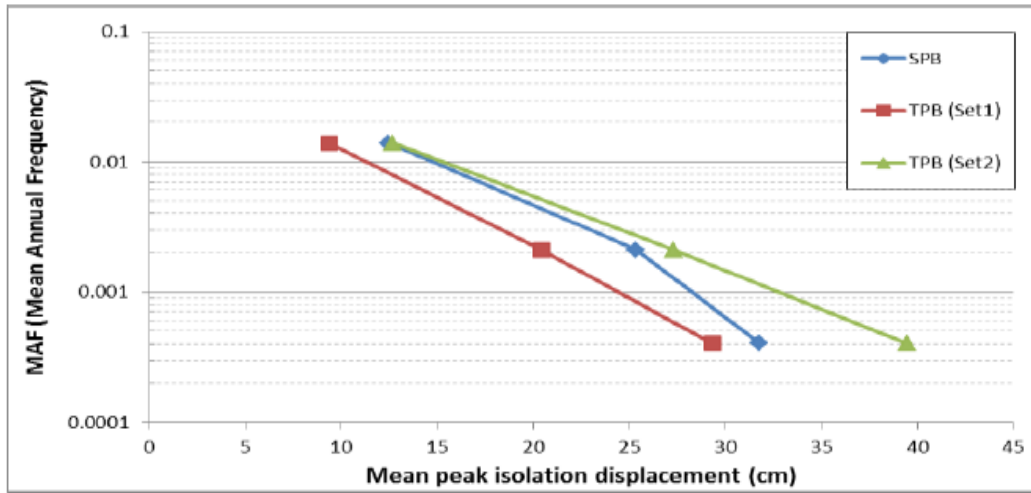


(a)



(b)

Continued



(c)

Fig. 6 Comparison of median demand parameters for two isolation systems

### 5.1 Performance of TPB Set 1 in comparison with SPB bearing

As shown in Fig. 6 TPB Set 1 has its most efficiency in constraining the isolator displacement comparing to SPB system than the shear force or sloshing displacement. The most efficient performance of TPB system in reducing shear force and sloshing displacement can be observed in SLE and DBE level earthquakes respectively. As seen, TPB Set 1 can mitigate all structure's responses in different levels of hazard in comparing to SPB systems.

### 5.2 Performance of TPB Set 2 in comparison with SPB bearing

In Fig. 6, at SLE level two types of isolation systems have approximately same response for three different demand parameters. Its reason can be explained by similar characteristic of TPB Set 2 and SPB systems in premier stages (Stage I and Stage II). In DBE level TPB Set 2 system has better performance than SPB system for decreasing mean normalized tower shear force.

Comparing the mean peak isolation displacement of both isolators in DBE and MCE level shows that lower stiffness in Stage III to IV of TPB system in compare to stiffness of SPB results higher peak isolation displacement. This result indicates in MCE level, the Stage V of TPB has not been activated to reduce the isolation displacement.

## 6. Conclusions

In this paper mathematical formulations involving complex nonlinear time history analysis have been proposed for analysis of the elevated liquid Storage tank isolated by the Triple Pendulum Bearing (TPB) subjected to multi hazard level excitation.

Simulating the behavior of isolated tank with two different isolation systems (SPB as well as TPB) under different hazard levels reveals the fact that the one with TPB bearing outperforms the

SPB. The results show that due to the varying adaptive behavior of TPB, it can significantly decrease the response of the structure (especially tower shear force) comparing to traditional type of friction pendulum bearing, SPB. It is also observed that different design strategy of TPB can change the efficiency of this system. Depends on the selected design strategy and seismic hazard level, there is possibility to observe higher peak isolation displacement in TPB than SPB system.

Due to above mentioned facts, Triple Pendulum Bearings in comparison to other types of isolators, can be widely applied on the elevated liquid tanks as an effective tool to control the response of these structures and satisfy the design demands.

## References

- Bleiman, D. and Kim, S. (1993), "Base isolation of high volume elevated water tanks", *Proceeding Seminar on Seismic Isolation, Passive Energy Dissipation, and Active Control*, ATC 17-1, Applied Technology Council, Redwood City, California.
- Christovasilis, I.P. and Whittaker, A.S. (2008), "Seismic analysis of conventional and isolated LNG tanks using mechanical analogs", *Earthq. Spectra*, **24**, 599-616.
- Fenz, D.M. and Constantinou, M.C. (2006), "Behaviour of the double concave friction pendulum bearing", *Earthq. Engng. Struct. Dyn.*, **35**(11), 1403-1422.
- Fenz, D.M. and Constantinou, M.C. (2008a), "Spherical sliding isolation bearings with adaptive behavior: theory", *Earthq. Eng. Struct. Dyn.*, **37**(2), 163-183.
- Fenz, D.M. and Constantinou, M.C. (2008b), "Spherical sliding isolation bearings with adaptive behavior: experimental verification", *Earthq. Eng. Struct. Dyn.*, **37**(2), 185-205.
- Fenz, D.M. and Constantinou, M.C. (2008c), "Modeling triple friction pendulum bearings for response history analysis", *Earthq. Spectra*, **24**(4), 1011-1028.
- Haroun, M.A. (1983), "Vibration studies and test of liquid storage tanks", *Earthq. Eng. Struct. Dyn.*, **11**, 179-206.
- Jadhav, M.B. and Jangid, R.S. (2006), "Response of base-isolated liquid storage tanks to near fault motions", *Struct. Eng. Mech.*, **23**, 615-634.
- Kelly, J.M. (1999), "The role of damping in seismic isolation", *Earthq. Eng. Struct. Dyn.*, **28**(1), 3-20.
- Knay, C.E. (1995), "Performance of elevated tanks during recent California seismic events", *AWWA Annual Conference & Exhibition*.
- Makris, N. and Vassiliou, M.F. (2011), "The existence of 'complete similarities' in the response of seismic isolated structures subjected to pulse-like ground motions and their implications in analysis", *Earthq. Eng. Struct. Dyn.*, **40**(10), 1103-1121.
- Malekzadeh, M. and Taghikhany, T. (2010), "Adaptive behavior of double concave friction pendulum bearing and its advantages over friction pendulum systems", *Scientia Iranica*, **17**(2), 81-88.
- Malekzadeh, M. and Taghikhany, T. (2012), "Multi-stage performance of seismically isolated bridge using triple pendulum bearings", *Adv. Struct. Eng.*, **15**(7), 1181-1196.
- Malhotra, P.K. (1997), "New method for seismic isolation of liquid-storage tanks", *Earthq. Eng. Struct. Dyn.*, **26**, 839-847.
- Minowa, C. (1980), "Dynamic analysis for rectangular water tanks", *Recent Adv. Lifeline Earthquake Engineering Japan*, 135-142.
- Morgan, T.A. (2007), "The use of innovative base isolation systems to achieve complex seismic performance objectives", Ph.D. Dissertation, Department of Civil and Environmental Engineering, University of California, Berkeley.
- Morgan, T.A. and Mahin, S.A. (2007), "Enhancing the performance capabilities of seismically isolated buildings using multi-stage friction pendulum sliding bearings", *Proc. World Forum on Smart Mat. And Smart Struct. Tech.*, Chongqing and Nanjing, China.

- Shampine, L.F. and Reichelt, M.W. (1997), "The MATLAB ODE suite", *SIAM J. Sci. Comput.*, **18**, 1-22.
- Shenton, III H.W. and Hampton, F.P. (1999), "Seismic response of isolated elevated water tanks", *J. Struct. Eng.* – ASCE, **125**(9), 965-976.
- Shrimali, M.K. and Jangid, R.S. (2003), "Earthquake response of isolated elevated liquid storage steel tanks", *J. Constr. Steel Res.*, **59**(10), 1267-1288.
- Somerville, P.D., Anderson, J., Sun, S.P. and Smith, N. (1998), "Generation of ground motion time histories for performance-based seismic engineering", *Proc. 6th National Earthq. Eng. Conf.*, Seattle, Washington.
- Sonia, D.P., Mistryb, B.B. and Panchala, V.R. (2011), "Double variable frequency pendulum isolator for seismic isolation of liquid storage tanks", *Nucl. Eng. Des.*, **241**, 700-713.
- Steinbrugge, K.V. and Rodrigo, F.A. (1963), "The Chilean earthquakes of May 1960: a structural engineering viewpoint", *Bull. Seismol. Am.*, **53**, 225-307.
- Wang, Y., Teng, M. and Chung, K. (2001), "Seismic isolation of rigid cylindrical tanks using friction pendulum bearings", *Earthq. Eng. Struct. Dyn.*, **30**, 1083-1099.

SA